Structural and functional studies of the enteropathogenic Escherichia coli type III needle complex protein EscJ

ARTICLE *in* MOLECULAR MICROBIOLOGY · APRIL 2005

Impact Factor: 4.42 · DOI: 10.1111/j.1365-2958.2005.04508.x · Source: PubMed

Molecular Microbiology (2005) **55**(6), 1658–1670 doi:10.1111/j.1365-2958.2005.04508.x

Structural and functional studies of the enteropathogenic *Escherichia coli* type III needle complex protein EscJ

Valérie F. Crepin,[1†] Sunil Prasannan,[2†] Rob K. Shaw,[3] Rebecca K. Wilson,[1] Elizabeth Creasey,[1] Cecilia M. Abe,[3] Stuart Knutton,[3] Gad Frankel[1] and Steve Matthews[2*]**

Centres for [1]Molecular Microbiology and Infection and [2]Structural Biology, Department of Biological Sciences, Imperial College London, London SW7 2AZ, UK.
[3]Institute of Child Health, University of Birmingham, Birmingham B4 6NH, UK.

Summary

The type III secretion system (TTSS) is a macromolecular structure that spans the cell wall of Gram-negative bacterial pathogens, enabling delivery of virulence effector proteins directly to the membranes and cytosol of host eukaryotic cells. TTSS consists of a conserved needle complex (NC) that is composed of sets of inner and outer membranes rings connected by a periplasmic rod. Enteropathogenic *Escherichia coli* (EPEC) is an extracellular diarrhoeagenic pathogen that uses TTSS to induce actin polymerization and colonizes the intestinal epithelium. In EPEC, EscJ is predicted to be targeted to the periplasm, in a *sec*-dependent manner, and to bridge the TTSS membrane-associated rings. In this study we determined the global fold of EscJ using Nuclear Magnetic Resonance spectroscopy. We show that EscJ comprises two subdomains (D1 – amino acid residues 1–55 in the mature protein, and D2 – amino acid residues 90–170), each comprising a three-stranded β-sheet flanked by two α-helices. A flexible region (residues 60–85) couples the structured regions D1 and D2. Periplasmic overexpression of $EscJ_{D1}$ and $EscJ_{D2}$ in a single *escJ* mutant bacterium failed to restore protein secretion activity, suggesting that the flexible linker is essential for the rod function. In contrast, periplasmic overexpression of $EscJ_{D1}$ and $EscJ_{D2}$ in the same wild-type bacterium had a dominant-negative phenotype suggesting defective assembly of the TTSS and protein translocation.

Accepted 1 December, 2004. For correspondences. *E-mail s.j.matthews@imperial.ac.uk; Tel. (+44) 207 594 5315; Fax (+44) 207 594 5207; **E-mail g.frankel@imperial.ac.uk; Tel. (+44) 20 7594 5253; Fax (+44) 20 7594 3069. †Both authors contributed equally to this paper.

Introduction

Enteropathogenic *Escherichia coli* (EPEC) is an extracellular Gram-negative pathogen and is the major cause of infantile diarrhoea in developing countries (Nataro and Kaper, 1998; Chen and Frankel, 2005). EPEC induces a characteristic histopathological lesion, termed the attaching and effacing (A/E) lesion, which is characterized by localized destruction of the intestinal brush border microvilli and intimate attachment of the bacterium to the host epithelial cell plasma membrane (Knutton *et al*., 1987; Frankel *et al*., 1998). During infection, EPEC injects effector proteins into the host cell via a type III secretion system (TTSS) and subverts the integrity of the host cell actin (Knutton *et al*., 1998; Campellone *et al*., 2004), microtubule (Matsuzawa *et al*., 2004) and intermediate filament (Batchelor *et al*., 2004) cytoskeletal networks and forms characteristic actin-rich pedestals underneath the attached bacterium (Knutton *et al*., 1989). The structural components of the EPEC TTSS are encoded in a pathogenicity island known as the locus of enterocyte effacement (LEE) (McDaniel *et al*., 1995; Elliott *et al*., 1998).

Type III secretion systems are utilized by many Gram-negative pathogens to directly translocate virulence factors into host cells (Hueck, 1998). The type III secretion apparatus is a multicomponent organelle assembled from the products of approximately 20 genes. Many components are broadly conserved among both virulence and flagellar TTSSs (Aizawa, 2001; Macnab, 2003). The secretion apparatus that can be isolated from bacterial membranes and visualized by transmission electron microscopy (TEM) is referred to as the needle complex (NC). Assembly of the NC occurs in stages (Sukhan *et al*., 2001; Marlovits *et al*., 2004); initially, in a *sec*-dependent manner, the membrane-bound components are exported to form the foundation of the NC. EscV in EPEC (Gauthier *et al*., 2003), PrgH in *Salmonella* (Kubori *et al*., 1998; Kimbrough and Miller, 2000; Kubori *et al*., 2000), MxiG in *Shigella* (Tamano *et al*., 2000; Blocker *et al*. 2001; Schuch and Maurelli, 2001) and YscV in *Yersinia* (Cornelis, 2002) form the inner membrane rings. InvG in *Salmonella*

(Kubori *et al*., 1998), MxiD in *Shigella* (Tamano *et al*., 2000; Blocker *et al*. 2001; Schuch and Maurelli, 2001), EscC in EPEC (Jarvis *et al*., 1995) and YscC in *Yersinia* (Koster *et al*., 1997), which belong to the secretin superfamily of outer membrane proteins, form the two outer membrane TTSS rings. Subsequently, the type III export machinery is assembled within the inner membrane and becomes associated with the base. Continued assembly of the NC occurs during the second, *sec*-independent phase, in which the type III export machinery, believed to be energized by an ATPase related to the catalytic subunits of bacterial F_0F_1 ATPases (Akeda and Galan, 2004), is utilized for the secretion of components constituting the 'needle' and more distal components of the apparatus. EscF (EPEC) (Wilson *et al*., 2001), PrgI (*Salmonella*) (Sukhan *et al*., 2003), YscF (*Yersinia*) (Marenne *et al*., 2003) and MxiH (*Shigella*) (Jouihri *et al*., 2003) form the needle component; EspA forms a filamentous extension to the needle component that is unique to the EPEC family of A/E lesion forming pathogens (Knutton *et al*., 1998).

The EPEC TTSS protein EscJ, which contains a *sec*-dependent signal sequence, is a highly conserved protein found in all TTSSs [e.g. PrgK in *Salmonella* (Kimbrough and Miller, 2000; Sukhan *et al*., 2001), MxiJ in *Shigella* (Allaoui *et al*., 1992; Schuch and Maurelli, 2001) and YscJ in *Yersinia* (Michiels *et al*., 1991; Allaoui *et al*., 1995)] and is also homologous to the FliF protein in the flagella structure (Ueno *et al*., 1994). It has been proposed that EscJ homologues span the periplasm linking the inner and outer membrane rings, either by the insertion of the acylated N-terminus in the inner or outer membrane or by interaction with outer membrane-bound components (Deng and Huang, 1999; Schuch and Maurelli, 2001). FliF is significantly larger than EscJ, and forms the flagella integral membrane (MS) ring and part of the proximal rod (Ueno *et al*., 1992; 1994). The EscJ family member in the *Salmonella* pathogenicity island 1 (SPI-1) TTSS, PrgK, is required for formation of the inner membrane rings (Kimbrough and Miller, 2000; Sukhan *et al*., 2001). Although expression of PrgK in *E. coli* does not result in the formation of a definitive structure (Kimbrough and Miller, 2000), when it is expressed with PrgH (a functional homologue of EscD and FliG) regular structures, identical in size and shape to the inner membrane rings of the SPI-1 TTSS, are formed in the inner membrane (Kimbrough and Miller, 2000).

Interactions between EscJ homologues and other TTSS proteins have been observed. In *Shigella*, MxiJ interacts with the outer membrane ring-forming protein, MxiD (Schuch and Maurelli, 2001). The flagella EscJ homologue, FliF, interacts with FliG, which is homologous to the EPEC protein EscD (Oosawa *et al*., 1994); however, this interaction requires the C-terminal region of FliF (Francis *et al*., 1992; Marykwas *et al*., 1996; Kihara *et al*., 2000) that is not present in EscJ implying no interaction with EscD in the EPEC TTSS, at least, not through the same domains. The aim of this project was to further characterize the structural protein EscJ, and to better understand the role it plays in the assembly of the EPEC NC.

Results

EscJ sequence analysis

The *escJ* gene encodes a protein of 190 amino acids with the first 19 N-terminal amino acids predicted to comprise the protein signal peptide. Based on this prediction the calculated mass of the mature protein is 18647 Da. EscJ exhibits similarity to a number of TTSS proteins from other bacteria including PrgK and SsaJ in *Salmonella* (Hensel *et al*., 1997; Kimbrough and Miller, 2000; Sukhan *et al*., 2001), MxiJ in *Shigella* (Allaoui *et al*., 1992; Schuch and Maurelli, 2001), YscJ in *Yersinia* (Michiels *et al*., 1991; Allaoui *et al*. 1995) and PscJ in *Pseudomonas* (Yahr *et al*., 1996) (Fig. 1). It also shows homology to the N-terminus of the FliF protein, which is proposed to form the MS basal ring complexes and part of the proximal periplasmic rod of the flagellar apparatus (Ueno *et al*., 1992; 1994).

EscJ homologues have two structural motifs: a hydrophobic lipoprotein signal peptide in addition to a hydrophobic stretch of 20–30 amino acids at their C-terminus, followed by basic residues. The lipid modification of the N-terminus suggests protein insertion into the bacterial outer membrane whereas the C-terminal hydrophobic domain is predicted to act as a stop transfer signal, anchoring the protein in the inner membrane. Analysis of the EscJ sequence reveals that while its homologues contain a consensus sequence (Leu–(Ala/Ser)–(Gly/Ala)–Cys) specifically recognized by the lipoprotein signal peptidase of the Sec-pathway (signal peptidase II) (Hayashi and Wu, 1990; Sankaran and Wu, 1994), EscJ contains an alternative sequence (Thr–Val–Ala–Cys) which is also predicted to be recognized as a lipoprotein signal sequence, by sequence analysis software (Prosite – http://c.expasy.org/prosite/; LipoP 1.0 – Juncker *et al*., 2003). The C-terminal domain of EscJ contains hydrophobic residues that might anchor the protein to the inner membrane although no transmembrane domain could be predicted with any certainty.

Cellular localization of EscJ

EscJ is predicted to be localized to the periplasm with a possible anchorage to both inner and outer membranes. Indeed, determining the distribution of EscJ in fractionated bacteria revealed that although the protein is mainly associated with the outer membrane it also fractionated with inner membrane markers (data not shown). Consistent with this, localization of EscJ by immunogold elec-

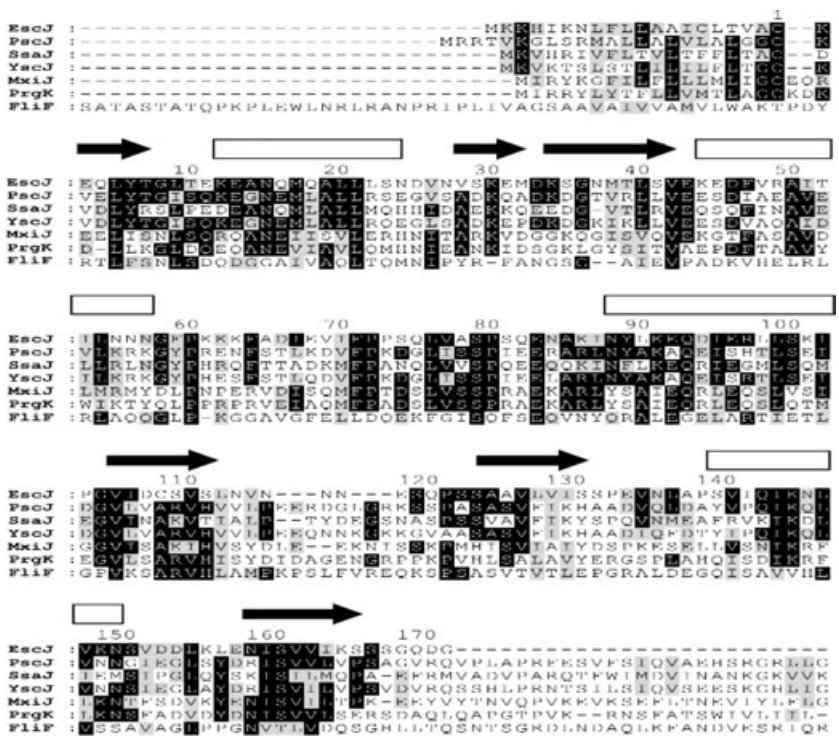

Fig. 1. Amino acid sequence alignment of EscJ homologues. EscJ amino acid sequence from EPEC (E2348/69) was aligned with putative TTSS apparatus proteins SsaJ (*Salmonella typhimurium* SPI-2), PscJ (*Pseudomonas aeruginosa*), YscJ (*Yersinia pestis*), MxiJ (*S. flexneri*), PrgK (*S. typhimurium* SPI-1) and FliF (*S. typhimurium*). Black regions correspond to identical amino acids or conserved residues present in >50% of sequences, dark grey indicates conserved substitutions and light grey indicates semi-conserved residues. Secondary structure assignments are provided above the sequence of EscJ, open boxes are α-helices and black arrows are β-strands. Numbering refers to the EscJ sequence and starts from the C+1 residue.

tron microscopy revealed that EscJ antiserum labels distinct regions of the EPEC membranes. In particular, EscJ was colocalized with the EspA filament that is built on the NC platform as well as in the septation furrow (Fig. 2), which has been shown to be the initial secretion site for *Shigella flexneri* Ipa proteins (Mounier *et al*., 1997).

The global fold of EscJ

Despite the unusually low number of aromatic residues (3% in total) and the associated poor chemical shift dispersion, >90% of ^{1}H, ^{15}N, $^{13}C\alpha$, $^{13}C\beta$, ^{13}CO and $^{1}H\alpha/\beta$, resonances could be assigned using the triple labelled $^{2}H/^{13}C/^{15}N$ sample (Fig. 3). The presence of conformational exchange within regions spanning 60–62 and 80–81, and a paucity of nuclear overhauser effects (NOEs) between the N-terminal and C-terminal halves of EscJ suggest the presence of two subdomains connected by a linker between residues 60 and 85. The consensus plot of chemical shift deviations from random coil values indicates that the linker region possesses little regular secondary structure with perhaps a propensity of extended β-structure between residues 65 and 70 and each subdomain is composed of mixed α/β topology (Fig. 4B).

In order to determine the global fold of EscJ, the mature protein (lacking the N-terminal 20 amino acids) was cloned into pET28a (generating plasmid pICC287) for

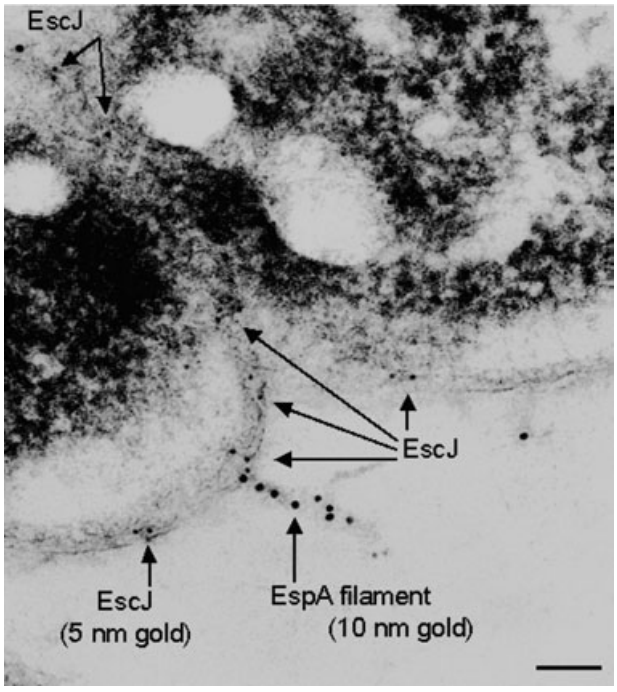

Fig. 2. EscJ localization by immunogold labelling. Immunogold labelling of EscJ on wild-type EPEC was performed using EscJ rabbit polyclonal antiserum and EspA mouse monoclonal antibodies were used to label EspA filaments, followed by anti-rabbit secondary antibodies coupled with 5 nm gold bead for EscJ and anti-mouse secondary antibodies coupled with 10 nm gold bead to label EspA. EscJ is shown to colocalize with the EspA filament on the NC platform as well as in the septation furrow. Bar represents 100 nm.

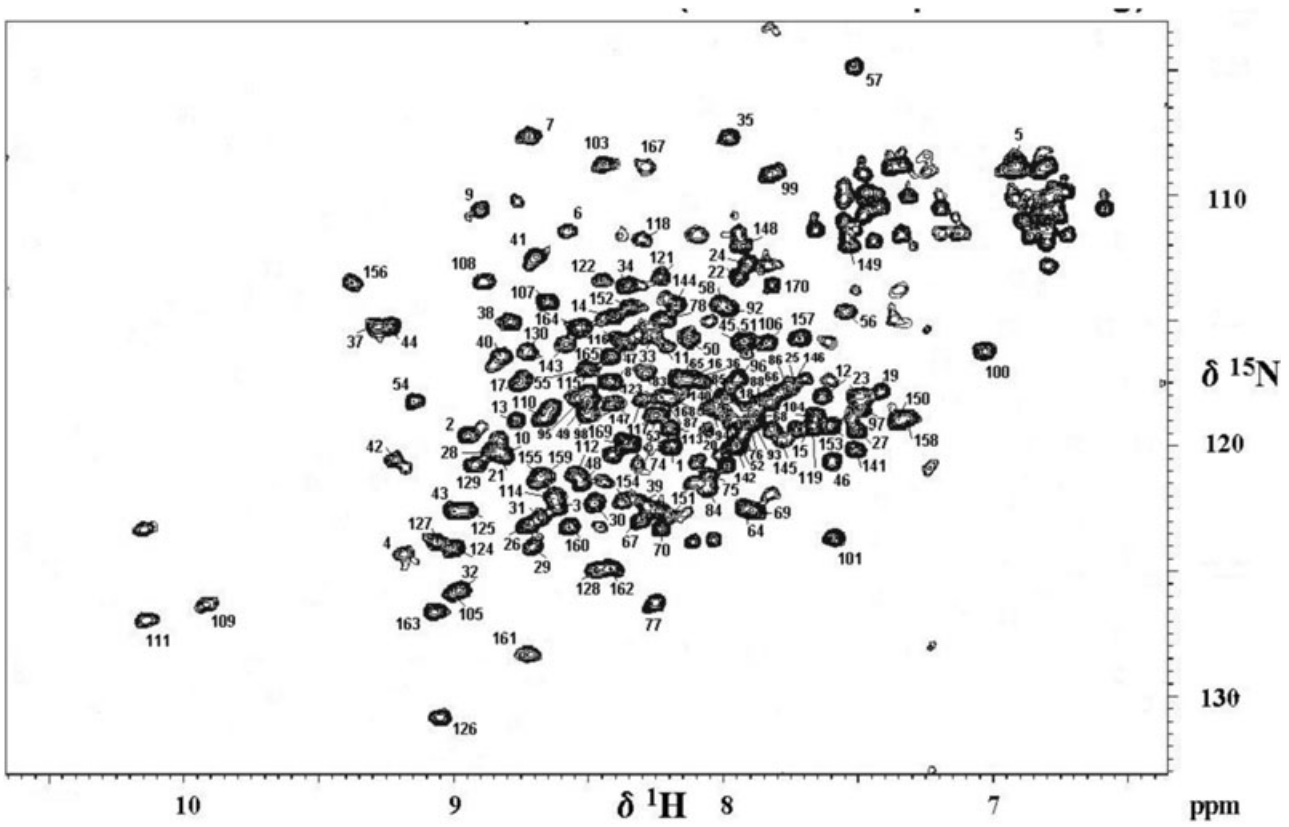

Fig. 3. Assigned ^{1}H–^{15}N HSQC NMR spectra of the EscJ. Sequential assignments of the backbone amides are indicated.

expression in *E. coli* BL21 as an N-terminal His-tagged protein. EscJ was purified by affinity chromatography, utilizing the Co^{2+} TALON resin. For Nuclear Magnetic Resonance (NMR), the pooled fractions were buffer exchanged with sodium phosphate buffer (pH 7.2) and concentrated to a final protein concentration of ≈250 μM. The global fold determination was based on three-dimensional (3D) NMR experiments performed on a ^{15}N,^{13}C,^{2}H triple-labelled sample of EscJ. These data were supplemented with information from a sample site-specifically ^{13}C/^{15}N labelled at Val, Leu and Ile side-chains. A total of 788 NOE-derived interproton distance constraints, 45 distance restraints for backbone hydrogen bonds, 93 dihedral angle restraints were used for the structure determination. The 10 lowest energy structures were chosen from a total of 100 calculated, based on agreement with experimental data and structural quality. No NOE violations greater than 0.5 Å and dihedral angle violations greater than 5° were tolerated.

The two structured subdomains, termed domains D1 and D2 hereafter, span residues 1–55 and 90–170 in mature EscJ (i.e. without signal peptide) and comprise a β-sheet flanked by two α-helices (Fig. 4A–D). The strand topology for both domains is illustrated in Fig. 4B and D. The D1 sheet consists of residues 2–6, 27–31 and 37–40. The two helices, residues 12–22 and 44–55, are approximately mutually orthogonal, one to either side of the sheet. The RMSD (final low-energy family of 10 structures) across the structured β-sheet and α-helices is 1.0 Å (Fig. 4C). D2 differs from D1 in that it is 20 residues longer than D1, and its β-sheet (residues 105–110, 123–128, 160–163) involves parallel pairing between the second and third strands (residues 123–128, and 160–163). The two helices, residues 90–101 and 139–148, are roughly parallel, to one side of the sheet. The loops connecting D2's regions of secondary structure are slightly more extensive, accounting for a higher secondary structure-wise RMSD of 1.6 Å (Fig. 4C). One region of D2, residues 131–138, lacked any backbone assignments in the NMR spectra, due to possible conformational flexibility, as well as the presence of two Pro residues.

An apparently flexible region (residues 60–85) that couples the structured sections, D1 and D2, is revealed by NMR dynamics data, i.e. low ^{1}H–^{15}N heteronuclear NOE values for this region indicates high degree of flexibility (Fig. 4E). Furthermore, a lack of interdomain NOE contacts between D1 and D2 implies that the two domains are tumbling in solution independently of one another. However, this does not rule out an intimate association of

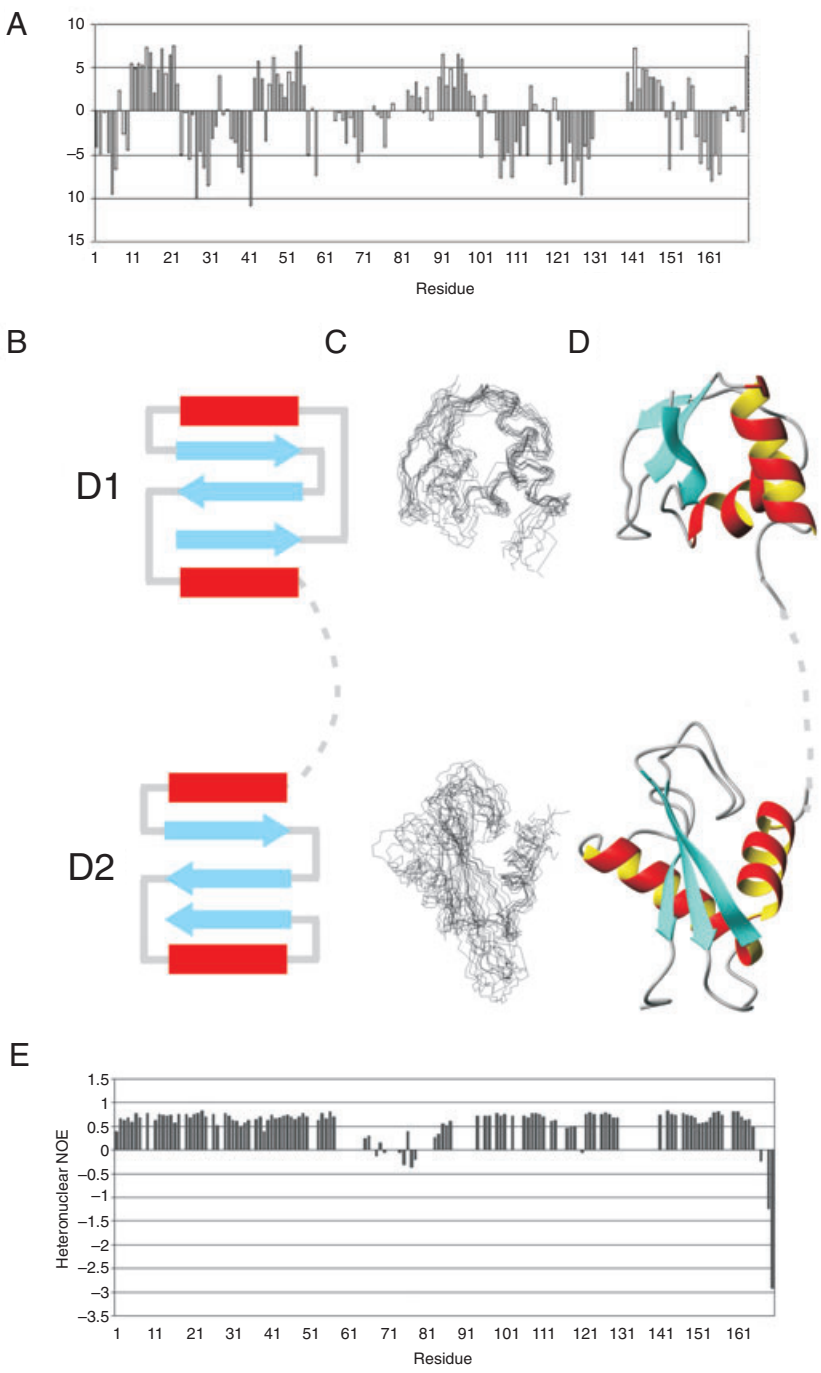

Fig. 4. The global fold of D1 and D2 from EscJ.
A. Consensus plot of the deviations from random coil $^{1}H_{\alpha}$, $^{13}C_{\alpha}$, $^{13}C_{\beta}$ and $^{13}C'$ chemical shifts.
B. Topology of D1 (top) and D2 (bottom) from EscJ. β-Strands are represented as blue arrows, α-helices are represented as red rectangles and the flexible D1–D2 linker is represented as a dashed grey line.
C. Backbone representation of the family of 10 lowest energy structures for D1 (top) and D2 (bottom).
D. Schematic representation of the folds of D1 (top) and D2 (bottom). β-Strands are shown in blue, α-helices are shown in red and the flexible D1–D2 linker is shown as a dashed grey line.
E. Plot of 2D ^{1}H–^{15}N steady-state heteronuclear NOE value against sequence number for AfaE-*dsc*.

the domains when EscJ is present within the secretion system complex. Atomic co-ordinates of both D1 and D2 were submitted to the Dali server (a network method for comparing protein structures in 3D) at the EMBL European Bioinformatics Institute (Holm and Sander, 1993; http://www.ebi.ac.uk/dali/). This revealed no significant structural homologues to either domain. The biological significance of this subdomain organization of EscJ was studied further.

Overexpression of EscJ domains D1 and D2 in ΔescJ *and wild-type EPEC strains*

The topology of EscJ revealed that the protein, in solution, is composed of two well-defined subdomains connected by a flexible linker. Based on the structure, we decided to investigate whether the covalent link between the two regions was indispensable for activity. The hypothesis was that if each domain could be expressed independently

from a specific vector then coexpression of the domains in the same bacterium would allow restoration of the function. For this purpose, constructs of the N-terminal domain (D1) and the C-terminal domain (D2) of EscJ have been engineered such that the EscJ native signal sequence was added at the 5′ (ssEscJ$_{D1}$ and ssEscJ$_{D2}$), in frame with the first amino acid of each domain. The two domains were then cloned into two vectors, pSA10 and pACYC184, with compatible origin of replication, ColE1 and p15A, generating plasmids pICC289 and pICC291 respectively. Transformation of either of the domains into an *escJ* mutant, strain ICC190, did not restore TTSS activity, as measured by lack of EspA filaments and A/E lesion formation (Fig. 5A). Co-transformation of pICC291 and pICC289 into ICC190, although resulted in comparable levels of ssEscJ$_{D1}$ and ssEscJ$_{D2}$, failed to complement protein

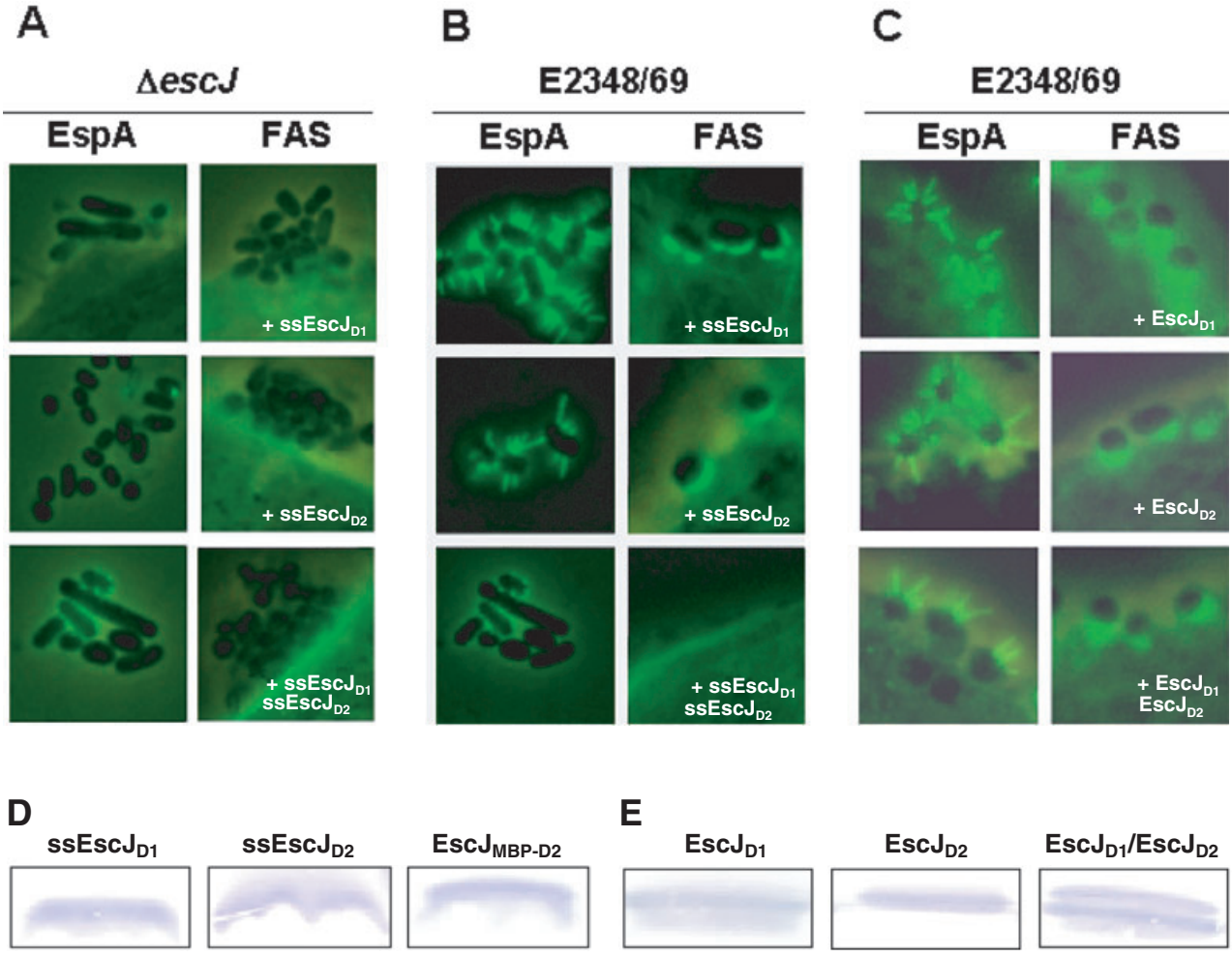

Fig. 5. Overexpression of EscJ-D1 and -D2 in Δ*escJ* and wild-type EPEC strains. Fluorescent action staining (FAS) assay and EspA staining were performed on Hep-2 cells infected with either wild-type E2348/69 EPEC or Δ*escJ* (ICC190) strains overexpressing EscJ-D1, -D2 or both domains, which contain the EscJ signal sequence [ssEscJ$_{D1}$ (pICC289) and ssEscJ$_{D2}$ (pICC291)] or without signal sequence [EscJ$_{D1}$ (pICC292) and EscJ$_{D2}$ (pICC294)]. Infections were performed in the presence of 1 mM IPTG.

A. Separate expression of ssEscJ$_{D1}$ and ssEscJ$_{D2}$ as well as coexpression of the two domains in Δ*escJ* strain did not complement the mutation. FAS assay was negative and no EspA filaments were detected on the surface of the bacterial cells.

B. The overexpression of ssEscJ$_{D1}$ or ssEscJ$_{D2}$ in wild-type EPEC did not affect the ability of the strain to produce EspA filaments and a FAS-positive assay. However, coexpression of the two domains (ssEscJ$_{D1}$ and ssEscJ$_{D2}$) in the same bacteria cell had a negative effect on A/E lesion formation and EspA filament expression.

C. Overexpression of cytosolic EscJ domains (EscJ$_{D1}$ and EscJ$_{D2}$) in wild-type EPEC had no effect as a wild-type phenotype was observed whether the domains were expressed separately or coexpressed in the same host.

D. Expression of ssEscJ$_{D1}$, ssEscJ$_{D2}$ and EscJ$_{MBP-D2}$ in E2348/69(pICC289), E2348/69(pICC291) and E2348/69(pICC296) respectively. Protein samples were prepared from cells crude extracts and the presence of EscJ domain was checked by Western blot, using EscJ rabbit polyclonal antiserum.

E. Expression of EscJ$_{D1}$, EscJ$_{D2}$ and coexpression of EscJ$_{D1}$/EscJ$_{D2}$ in E2348/69(pICC292), E2348/69(pICC294) and E2348/69(pICC292 + pICC294) respectively. Protein samples were prepared from cells crude extracts and the presence of EscJ domains was checked by Western blot, using EscJ rabbit polyclonal antiserum.

secretion (data not shown), EspA filament production and A/E lesion formation (Fig. 5A). This suggests that the function of EscJ is dependent on the two domains being covalently linked. We next tested whether expression of the domains in E2348/69 (Fig. 5D) would interfere with the activity of intact EscJ and have a dominant-negative phenotype. Overexpression of $ssEscJ_{D1}$ or $ssEscJ_{D2}$ did not affect the A/E lesion forming activity of E2348/69(pICC289) or E2348/69(pICC291) strains (Fig. 5B). In contrast, coexpression of $ssEscJ_{D1}$ and $ssEscJ_{D2}$ in E2348/69(pICC289 + pICC291) had a detrimental effect on A/E lesion formation (Fig. 5B). Elongation of EspA filaments was also impaired when the two domains were coexpressed in E2348/69(pICC289 + pICC291) (Fig. 5B), suggesting that the NC was not functional. Although having the native signal peptide attached to both $ssEscJ_{D1}$ and $ssEscJ_{D2}$ might interfere with domain localization within the periplasm, it is more likely that the N-terminus is targeted to the outer membrane while the C-terminus is associated with the inner membrane. Nevertheless, in order to eliminate the possibility of $ssEscJ_{D2}$ mislocalization when fused to the EscJ native signal sequence, we fused $EscJ_{D2}$ to the *sec* maltose-binding protein (MBP) signal sequence ($EscJ_{MBP\text{-}D2}$; Fig. 5D). Periplasmic localization of $EscJ_{MBP\text{-}D2}$ was confirmed by cell fractionation (data not shown). Overexpression of $EscJ_{MBP\text{-}D2}$ did not affect the A/E lesion forming activity of E2348/69(pICC296) whereas coexpression of $ssEscJ_{D1}$ and $EscJ_{MBP\text{-}D2}$ in E2348/69(pICC296 + pICC289) had a detrimental effect on A/E lesion formation (data not shown).

In order to confirm that the observed phenotype did not simply result from the overexpression, we repeated the same experiments but overexpressed $EscJ_{D1}$ and $EscJ_{D2}$ without the signal sequence, i.e. within the bacterial cytosol (plasmids pICC292 and pICC294, respectively; Fig. 5E). In those conditions, coexpression of $EscJ_{D1}$ and $EscJ_{D2}$ in E2348/69(pICC292 + pICC294) had no effect on the biogenesis EspA filaments or A/E lesion formation (Fig. 5C). This would suggest that, when targeted to the periplasm, $EscJ_{D1}$ and $EscJ_{D2}$ could compete with native EscJ for binding to other structural components and blocking formation of the NC. In addition, complementing ICC190 with a wild-type *escJ* clone (pICC288) restore function, but complementing ICC190 with a cytosolic EscJ (pICC297) lacking the secretion signal did not (data not shown).

Discussion

The TTSS NCs are multicomponent organelles elaborated on the bacterial cell surface. These organelles are large and complex, consisting of many different proteins and hundreds of individual subunits. Before their assembly, each subunit must first be targeted to its point of incorporation within a growing structure. In this paper we report structural and functional studies of the EPEC TTSS protein EscJ.

EscJ contains a *sec*-dependent signal sequence and is homologous to PrgK, MxiJ and YscJ, which are membrane-anchored proteins, extend to the periplasm and are structural components of their respective NCs (Hueck, 1998; Tampakaki *et al*., 2004). This family of proteins shares sequence similarity with the N-terminal region from the flagellar protein FliF. FliF polymerizes to form the inner membrane MS rings of the flagellar basal body with diameters of 30 nm (outer M ring) and 15 nm (inner S ring) and a short proximal rod (Ueno *et al*., 1992; 1994). Like the other members of the family, the MS ring also contains a central pore, which has been shown to house type III export components conserved between the flagellar and virulence-associated TTSS.

Structural analysis of the *Salmonella* NC had recently revealed that PrgK is associated with the inner membrane rings while the periplasmic rod is mainly composed of PrgJ (Marlovits *et al*., 2004). Significantly, no PrgJ homologue is present in EPEC and the combined PrgK/J function might be amalgamated in a single EPEC protein, EscJ. Indeed, cell fractionation had shown that unlike PrgK, EscJ is mainly associated with the outer membrane, while some is co-fractionated with inner membrane markers. In addition, the region of homology shared between FliF and EscJ (Fig. 1) is contained within the domain of FliF that is believed to line the central pore of the ring and proposed to form part of the proximal rod structure. This suggests that EscJ could form the cylindrical structure functioning as a bridge across the periplasmic space, connecting the outer and inner membrane rings of the NC, which is required for secretion of more distal apparatus components across the inner membrane. Electron microscopy (EM) analyses showed that EscJ is localized at the base of the nascent EspA filament, which is the filamentous extremity of the NC. Although EscJ does not present the lipobox consensus sequence (Leu–(Ala/Ser)–(Gly/Ala)–Cys) at positions –3 to +1 of its cleavage site, the EscJ sequence Thr-Val-Ala-Cys (–3 to +1) is nevertheless predicted to be a signature for lipoprotein. The Leu–(Ala/Ser)–(Gly/Ala)–Cys consensus sequence of the lipobox (also called lipoprotein box) represents the cleavage region of about 75% of all lipoprotein signal sequences in bacteria (Hayashi and Wu, 1990). EscJ would therefore belong to the 25% of lipoproteins that have an alternative signal sequence. In addition, the outer membrane localization of EscJ is in agreement with the '+2 rule', which has been proposed for the sorting of lipoproteins between the periplasmic faces of the bacterial cytoplasmic and outer membranes (Gennity and Inouye, 1991; Gennity *et al*., 1992; Seydel *et al*., 1999). An aspartate residue in position +2 has been shown to be responsible for specific

cytoplasmic membrane retention of lipoproteins whereas lipoproteins with lysine or glutamic acid at position +2 are more likely to be displaced to the outer membrane (Gennity and Inouye, 1991; Seydel *et al*., 1999). Moreover, YscJ and MxiJ, the *Yersinia* and *Shigella* homologues of EscJ, which contain lysine and glutamic acid residue in position +2, respectively, are likely to have the N-terminal part anchored into the outer membrane by its lipid moiety (Allaoui *et al*., 1992). The C-terminus is likely to be anchored to the inner membrane.

In flagellar biosynthesis, following MS ring formation, a C ring (for Cytoplasmic ring), is formed at the cytoplasmic face of the MS ring, which regulates the reversal frequency of the motor rotation (Hueck, 1998; Macnab, 2004). The C ring comprises FliN, FliG and FliM, which are proteins associated with the bacterial membrane and where FliG functions as a linker between FliF and a complex formed by FliN and FliM (Hueck, 1998). No homologues of FliM are found in TTSSs, whereas FliN is related to the members of the YscQ family of TTSS proteins (no homologue found in EPEC) and FliG belongs to the YscD protein family of which EscD is an EPEC homologue (Oosawa *et al*., 1994; Hueck, 1998). Therefore, YscJ homologues are speculated to interact with members of the YscQ and YscD families. While EscJ is likely to be the only TTSS protein spanning the periplasmic space, FliF is accompanied by other proteins forming the rod structure (FliE, FlgB, C, F and G), which connects the MS ring to the flagellar hook (Hueck, 1998; Saijo-Hamano *et al*., 2004). None of these proteins have homologues in EPEC. In addition, other structural proteins, which participate in rod formation and are likely to interact with the MS ring structure, are integral inner membrane proteins with periplasmic extensions, such as FliP, FliQ, FliR, FlhB and FlhA, whose homologues in EPEC are EscR, S, T, U and V respectively (Tampakaki *et al*., 2004). Recent studies carried out in our lab using the yeast two-hybrid system did not reveal any potential interactions involving EscJ and other structural components of the TTSS (Creasey *et al*., 2003). This system, however, may not be suitable to study membrane protein interactions and other methods would be required in order to identify EscJ partners.

By employing triple-labelled and specifically protonated samples of EscJ, as well as an appropriate suite of NMR experiments, we determined the global fold of the mature form of EscJ. We believe that this is the first structural insight into a component of the EPEC TTSS, as previous structural work mainly involved EM of the whole secretion apparatus (Daniell *et al*., 2001; Wilson *et al*., 2001). Although there are high-resolution crystal structures of FliN (PDB code: 1O6A), the C-terminal domain of FliG (PDB code: 1LKV) and FliC (PDB code: 1UCU), we understand that there are no current structures of EscJ homologues.

The topology of EscJ in solution exhibits two principal subdomains, which we termed domains $EscJ_{D1}$ and $EscJ_{D2}$. Sequence alignment with key EscJ homologues and FliF reveals that the secondary structure elements are largely conserved (Fig. 1). Furthermore, the linker region connecting $EscJ_{D1}$ and $EscJ_{D2}$ contains a stretch between residues 71 and 80 that is also highly conserved. Although these domains appear to be independent in solution, the conservation within this region may imply the formation of a more globular, compact structure when EscJ is incorporated into the secretion system complex. Alternatively, this region could be important in EscJ oligomerization or its interaction with other components of the TTSS complex.

No phenotype was seen when the domains were individually expressed in wild-type EPEC. Expressing either $EscJ_{D1}$ or $EscJ_{D2}$ in ICC190 did not complement the *escJ* mutation, indicating that in isolation the subdomains are not able to oligomerize to form a functional protein. The linker bridging the two structured regions is therefore essential for proper secretion of translocator and effector proteins via the TTSS. This could point to the linker acting as a flexible means of controlling the aperture of the channel, and thereby protein secretion through the NC. Otherwise, the absence of the linker could destabilize EscJ oligomerization and interactions with partner proteins, thereby disrupting the bridge between the inner membrane and outer membrane ring structures. Interestingly, periplasmic coexpression of $EscJ_{D1}$ and $EscJ_{D2}$ in wild-type EPEC, using either the native EscJ signal peptide or a combination of EscJ and MBP signal peptide, had a dominant-negative effect, as the strain was unable to form A/E lesions and no EspA filaments were produced, while cytoplasmic coexpression of the EscJ domain in the same wild-type bacterium had no inhibitory effect. Thus, although the subdomains are not capable of mimicking EscJ if they are not covalently linked, they are likely to interact with the native EscJ in a competitive manner. Because the two fragments were overexpressed and therefore more abundant in the cell than the native EscJ, one can postulate that the heterodimer took over EscJ, impairing the structure of the channel and resulting in the formation of non-functional secretion machinery.

In this study, we have reported the first structure of a component of the EPEC TTSS. By sequence analysis, we have drawn parallels between EscJ and its homologues in other TTSSs and using structural and molecular analysis, we have confirmed the role and the localization of EscJ within the NC and shown that the integrity of the protein is necessary for the formation of the periplasmic channel connecting the outer and inner membrane rings of the basal structure of the EPEC type III secretion machinery.

Experimental procedures

Bacterial strains and growth conditions

The plasmids and bacterial strains used in this study are listed in Table 1. Bacteria were grown in Luria–Bertani (LB) medium or in Dulbecco's modified Eagle's medium (DMEM) supplemented with ampicillin (100 μg ml^{-1}), kanamycin (50 μg ml^{-1}) and chloramphenicol (34 μg ml^{-1}) as required. Strain E2348/69 Δ*escJ* (ICC190; Table 1) was constructed using a modified version of the λ Red recombinase expression method described by Mundy *et al*. (2004). The *escJ* gene and flanking regions were polymerase chain reaction (PCR)-amplified, from E2348/69 genomic DNA using the pairs of primers escJ-flank1-Fw, escJ-flank1-Rv (amplifying the flanking region 1, in 5′ of *escJ*) and escJ-flank2-Fw, escJ-flank2-Rv (amplifying the flanking region 2, in 3′ of *escJ*) (Table S1). The escJ-flank1-Rv and the escJ-flank2-Fw primers contain a *Bam*HI site in their sequence, allowing ligation of the two PCR products (flanking 1 and flanking 2) following *Bam*HI digestion, which fragment was then cloned into pGEMT-easy vector. The non-polar *aphT* cassette (Galan *et al*., 1992), which confers kanamycin resistance, was inserted into pGEMT-easy derivative in the *Bam*HI site between *escJ* flanking 1 and flanking 2. After verifying for correct orientation of the kanamycin cassette, the [flanking 1–*aphT*–flanking 2] fragment was PCR-amplified using escJ-flank1-Fw and escJ-flank2-Rv primers. The PCR product was electroporated in E2348/69, which contains the pKD46 plasmid encoding for the λ Red recombinase. Transformants were selected on kanamycin plates and the mutation was confirmed by PCR.

Cloning of EscJ and EscJ domains

To complement the *escJ* mutant, *escJ* gene was PCR-amplified from E2348/69 genomic DNA using the EcoRI-escJ-Fw and SmaI-escJ-Rv primers (Table S1). The PCR product was cloned in pSA10 under the IPTG-inducible P*tac* promoter, creating the pICC288 vector (Table 1). ssEscJ-D1 and -D2 were amplified by inverse-PCR using pICC288 as DNA template. The primer pairs [escJ-D1-Fw1/escJ-D1-Rv1] and [escJ-D2-Fw1/escJ-D2-Rv1] (Table S1) were designed to amplify ssEscJ-D1 and -D2, respectively, such that the native EscJ signal sequence was fused to the N-terminus of each domains. The inverse-PCR fragments were then circularized to create pICC289 and pICC290 vectors (Table 1). In order to coexpress the two domains in the same bacterial host ssEscJ-D2 was subcloned, together with the P*tac* promoter, in a *Bam*HI-digested pACYC184 vector, creating the pICC291 plasmid. EscJ-D2 fused to the MBP *sec* signal sequence was PCR-amplified from E2348/69 genomic DNA using the [escJ-D2-Fw3/SmaI-escJ-Rv] primers (Table S1). The PCR product was *Eco*RI/*Sma*I digested and cloned in pSA10 then *Bam*HI subcloned in pACYC184 as described above, generating pICC295 and pICC296 vectors respectively (Table 1). Similarly, EscJ, EscJ-D1 and -D2 without the native EscJ signal sequence were PCR-amplified using the primer pairs [escJ-D1-Fw2/SmaI-escJ-Rv], [escJ-D1-Fw2/escJ-D1-Rv1] and [escJ-D2-Fw2/SmaI-escJ-Rv] (Table S1). The PCR fragments were *Eco*RI/*Sma*I digested and cloned into pSA10, generating pICC292 and pICC293 plasmids (Table 1). EscJ-D2 was subcloned in pACYC184 as described above, generating the pICC294 vector (Table 1). In all constructs, expression of recombinant proteins was driven by the IPTG-inducible P*tac* promoter of the pSA10 vector.

In order to purify the mature form of EscJ, *escJ* gene lacking the signal sequence was PCR-amplified from E2348/69 genomic DNA using the NdeI-escJ-Fw and HindIII-escJ-Rv primers (Table S1). Primers were designed to generate an in-frame fusion protein with the six Histidines N-terminal tag present on the pET28a expression vector. The PCR product was *Nde*I/*Hin*dIII digested before it was ligated into pET28a, generating pICC287 plasmid, where expression of the gene is driven by the IPTG-inducible T7 promoter.

Table 1. Strains and plasmids used in this study.

	Description	Source of reference
Strains		
E2348/69	Wild-type EPEC O127:H6	Levine *et al*. (1985)
BL21 pLysS	Host for protein expression from T7 promoter	Novagen
ICC190	Δ*escJ*::Km in E2348/69	This study
Plasmids		
pET28a	Expression vector	Novagen
pACYC184	Expression vector	New England Biolabs
pGEMT-easy	Cloning vector	Promega
pKD46	Coding for the λ Red recombinase	Datsenko and Wanner (2000)
pSA10	Expression vector, pKK177-3 derivative containing *lacI* gene	Schlosser-Silverman *et al*. (2000)
pICC287	pET28a-EscJ	This study
pICC288	pSA10-EscJ (native EscJ)	This study
pICC289	pSA10-ssEscJ-D1 (with EscJ signal sequence)	This study
pICC290	pSA10-ssEscJ-D2 (with EscJ signal sequence)	This study
pICC291	pACYC184-ssEscJ-D2 (with EscJ signal sequence)	This study
pICC292	pSA10-EscJ-D1 (without EscJ signal sequence)	This study
pICC293	pSA10-EscJ-D2 (without EscJ signal sequence)	This study
pICC294	pACYC184-EscJ-D2 (without EscJ signal sequence)	This study
pICC295	pSA10-EscJ-MBP-D2 (with MBP signal sequence)	This study
pICC296	pACYC184-EscJ-MBP-D2 (with MBP signal sequence)	This study
pICC297	pSA10-EscJ (without EscJ signal sequence)	This study

Expression, purification and labelling of EscJ for NMR work

The expression of EscJ from pICC287 vector was carried out in BL21 DE3 cells. Cell cultures were grown at 37°C to $OD_{600} \approx 0.5$. EscJ protein expression was then induced by adding 0.4 mM IPTG and the cells grown for 4 h at 30°C. Different growth media were used for specific labelling of EscJ. EscJ labelling with ^{13}C and ^{15}N isotopes was performed in minimal medium, consisting of 6 g l^{-1} Na_2HPO_4, 3 g l^{-1} KH_2PO_4, 0.5 g l^{-1} NaCL, 0.7 g l^{-1} [15-N]-NH_4Cl as well as 1 ml l^{-1} trace element stock solution, 1 ml l^{-1} 1 M $MgSO_4$, 1 ml l^{-1} 0.1 M $CaCl_2$, 1 ml l^{-1} 1 M thiamine and 0.2% [^{13}C]-D-glucose. Perdeuteration with $^{13}C/^{15}N$ labelling was achieved by expressing EscJ in triple-labelled medium OD1 CDN (Silantes). Specific $^{13}C/^{15}N$ labelling at Val, Leu and Ile residues was obtained by expressing EscJ protein in the minimal medium as described above, but by substituting with unlabelled D-Glucose, and adding 1 g l^{-1} uniformly [$^{13}C/^{15}N$]-Val and [$^{13}C/^{15}N$]-Ile; labelled Leu was derived via the Val biosynthetic pathway, although this resulted in backbone carbon atoms not being labelled.

Following induction, bacteria cells were harvested by centrifugation at 8000 *g* for 15 min at 4°C, the pellets resuspended in lysis buffer (50 mM NaH_2PO_4, 300 mM NaCl, 10 mM Imidazole; pH 8.0) and cells disruption was achieved via sonication. The sample was centrifuged at 10 000 *g* for 10 min to remove cellular debris. The fusion protein was purified by affinity chromatography, using a Co^{2+} TALON metal affinity resin (Becton-Dickinson). Sample (20 ml) was added to 2 ml of TALON resin, and left to incubate at room temperature for 20 min with shaking before centrifuging at 700 *g* for 5 min. The supernatant was discarded and the resin washed twice with 20 ml of lysis buffer for 15 min at room temperature. The washed resin was added to a 10 ml column and EscJ was eluted with 20 ml elution buffer (50 mM NaH_2PO_4, 300 mM NaCl, 0.5 M Imidazole; pH 8.0). For NMR, the pooled fractions were buffer exchanged (1 in 10) with sodium phosphate buffer (pH 6.5) by centrifugation at 3000 *g* using 20 ml Vivaspin concentrators (Vivascience).

Nuclear magnetic resonance spectroscopy and structure calculation

Nuclear magnetic resonance spectra were recorded on a Bruker DRX-500 shielded 500 MHz spectrometer. All experiments were carried out at 303 K. Two-dimensional (2D) ^1H–^{15}N heteronuclear single quantum coherence (HSQC) spectra were recorded to pick backbone amide resonances, and triple resonance (^1H,^{15}N,^{13}C) spectra used to sequentially assign these peaks (reviewed in Sattler *et al*., 1999). Experiments included the HNCA, HN(CO)CA, CBCA(CO)NH, HNCACB, HNCO and HN(CA)CO (reviewed in Sattler *et al*., 1999). Most of the above were recorded in their deuterated-optimized form on the deuterated sample of EscJ to complete backbone resonance assignment. Subsequently, the HBHA(CBCACO)NH (recorded on a non-deuterated sample) and HCCH-TOCSY (recorded on the specifically [^{13}C]-Val/Ile/Leu-labelled sample) experiments were used to assign side-chain H_β, and Val/Ile/Leu methyl groups respectively.

Nuclear overhauser effect data, yielding interproton distance information, were obtained by recording ^1H–^{15}N NOESY-HSQC and ^1H–^{15}N HMQC-NOESY-HSQC spectra on the deuterated EscJ sample (backbone-backbone NOEs) and the non-deuterated sample (α-proton/β-proton to backbone NOEs). Side-chain to side-chain/α/β/amide proton NOEs were obtained by recording a ^1H–^{13}C NOESY-HSQC on the specifically [^{13}C]-Val/Ile/Leu-labelled sample.

Values for backbone torsion angles (Phi/Psi) were obtained via the algorithm TALOS (Cornilescu *et al*., 1999). Ninety-three sets of good predictions were used in the subsequent structure calculation (for a total of 186 individual angles).

Locations of hydrogen bonds were based on predicted locations of secondary structure, based loosely on stretches of α-helix or β-sheet predicted by the TALOS Phi/Psi values obtained above. Forty-five sets of HN-O and N-O distances were incorporated into the structure calculation distances.

Preparation of EscJ polyclonal antiserum and Western blot analysis

His-EscJ was purified from induced BL21(pICC287) culture as described (Neves *et al*., 2003). The purified protein was used to generate polyclonal EscJ antiserum as described (Neves *et al*., 2003).

For Western blot analysis, EPEC bacteria were grown in 15 ml of DMEM at 37°C with shaking for 6 h. Bacterial cells from an equal volume of culture were pelleted by centrifugation at 8000 *g* for 10 min, and resuspended in ($OD_{600} \times 200$) µl of loading buffer. An equal volume of samples was loaded and separated by SDS-12% PAGE followed by Western blotting using EscJ rabbit polyclonal antiserum. Immunoblots were developed by the addition of one buffered substrate tablet (Sigma) containing 0.15 mg l^{-1} 5-bromo-4-chloro-3-indolyl phosphate and 0.30 mg l^{-1} nitroblue tetrazolium dissolved in 10 ml of distilled water. Membranes were developed simultaneously.

Bacterial infection of HEp-2 cells and immunofluorescence analysis

Subconfluent cultures of HEp-2 cells on glass coverslips were placed in wells of a 24-well tissue culture plate containing 1 ml of Hepes-buffered minimal essential medium containing 2% fetal calf serum, in the presence or absence of 1 mM IPTG. Ten microlitres of an overnight bacterial broth culture were added to each well, and the cells were incubated for 3 h at 37°C. Non-adherent bacteria were removed with a mild wash with DMEM and coverslips were fixed in 4% buffered formalin pH 7.3 for 20 min. All staining and wash procedures were performed using phosphate-buffered saline (PBS) blocking buffer pH 7.3 containing 0.2% bovine serum albumin. Washed cells were permeabilized by treating coverslips with 0.1% Triton X-100 in PBS for 5 min. After three PBS washes, coverslips were incubated with a solution of fluorescein isothiocyanate-phalloidin (5 µg ml^{-1}; Sigma) in PBS for 20 min to stain filamentous cell actin. To stain EspA filaments, coverslips were stained with polyclonal $EspA_{EPEC}$ antibody for 45 min. Following three washes, coverslips were labelled for 45 min with 1:100 GAR Alexa488 fluorescent conjugate

(Molecular Probes). Coverslips were mounted and examined on a Leica DMRE microscope, equipped with a digital camera system.

Immunogold labelling

For TEM, overnight bacterial culture grown at 37°C in LB broth was diluted 1:100 in DMEM (Sigma) and incubated for 4 h, at 37°C. Samples were then fixed with 0.5% glutaraldehyde and 2% paraformaldehyde in 0.1 M PBS, dehydrated through a graded series of ethanol (50, 75, 85, 95 and 100%) and embedded as a pellet in unicryl resin (BBInternational).

Ultra-thin sections placed onto Formvar-coated nickel grids were blocked with phosphate buffer containing 1% BSA (PBS-BSA) and first labelled with mouse anti-EspA and rabbit anti-escJ serum (primary antibodies – 1:100 dilution) for 1 h, at room temperature. After washing with PBS-BSA, samples were labelled with 5 nm gold-labelled goat anti-rabbit serum and 10 nm gold-labelled goat anti-mouse (secondary antibodies – 1:50 dilution) (British BioCell International) for 1 h, at room temperature. Grids were then washed with PBS-BSA and water, stained with 2% uranyl acetate and lead citrate and examined in a JEOL 1200EX transmission electron microscope operated at 80 kV.

Acknowledgements

This study was supported by the Wellcome Trust.

Supplementary material

The following material is available from
http://www.blackwellpublishing.com/products/journals/suppmat/mmi/mmi4508/mmi4508sm.htm
Table S1. Primers used in this study.

References

Aizawa, S.I. (2001) Bacterial flagella and type III secretion systems. *FEMS Microbiol Lett* **202:** 157–164.

Akeda, Y., and Galan, J. (2004) Genetic analysis of the *Salmonella enterica* type III secretion-associated ATPase InvC defines discrete functional domains. *J Bacteriol* **186:** 2402–2412.

Allaoui, A., Sansonetti, P., and Parsot, C. (1992) MxiJ, a lipoprotein involved in secretion of *Shigella* Ipa invasins, is homologous to YscJ, a secretion factor of the *Yersinia* Yop proteins. *J Bacteriol* **174:** 7661–7669.

Allaoui, A., Schulte, R., and Cornelis, G.R. (1995) Mutational analysis of the *Yersinia enterocolitica virC* operon: characterization of yscE, F, G, I, J, K required for Yop secretion and yscH encoding YopR. *Mol Microbiol* **18:** 343–355.

Batchelor, M., Guignot, J., Patel, A., Cummings, N., Cleary, J., Knutton, S., *et al.* (2004) Involvement of the intermediate filament protein cytokeratin-18 in actin pedestal formation during EPEC infection. *EMBO Rep* **5:** 104–110.

Blocker, A., Jouihri, N., Larquet, E., Gounon, P., Ebel, F., Parsot, C., *et al.* (2001) Structure and composition of the *Shigella flexneri* 'needle complex', a part of its type III secreton. *Mol Microbiol* **39:** 652–663.

Campellone, K., Robbins, D., and Leong, J. (2004) EspF(U) is a translocated EHEC effector that interacts with Tir and N-WASP and promotes Nck-independent actin assembly. *Dev Cell* **7:** 217–228.

Chen, H.D., and Frankel, G. (2005) Enteropathogenic *Escherichia coli*: unravelling pathogenesis. *FEMS Microbiol Rev* (in press).

Cornelis, G. (2002) The *Yersinia* Ysc-Yop virulence apparatus. *Int J Med Microbiol* **291:** 455–462.

Cornilescu, G., Delaglio, F., and Bax, A. (1999) Protein backbone angle restraints from searching a database for chemical shift and sequence homology. *J Biomol NMR* **13:** 289–302.

Creasey, E.A., Delahay, R.M., Daniell, S.J., and Frankel, G. (2003) Yeast two-hybrid system survey of interactions between LEE-encoded proteins of enteropathogenic *Escherichia coli*. *Microbiology* **149:** 2093–2106.

Daniell, S.J., Takahashi, N., Wilson, R., Friedberg, D., Rosenshine, I., Booy, F.P., *et al.* (2001) The filamentous type III secretion translocon of enteropathogenic *Escherichia coli*. *Cell Microbiol* **3:** 865–871.

Datsenko, K.A., and Wanner, B.L. (2000) One-step inactivation of chromosomal genes in *Escherichia coli* K12 using PCR products. *Proc Natl Acad Sci USA* **97:** 6640–6645.

Deng, W., and Huang, H. (1999) Cellular locations of *Pseudomonas syringae* pv. *syringae* HrcC and HrcJ proteins, required for harpin secretion via the type III pathway. *J Bacteriol* **181:** 2298–2301.

Elliott, S.J., Wainwright, L.A., McDaniel, T.K., Jarvis, K.G., Deng, Y.K., Lai, L.C., *et al.* (1998) The complete sequence of the locus of enterocyte effacement (LEE) from enteropathogenic *Escherichia coli* E2348/69. *Mol Microbiol* **28:** 1–4.

Francis, N., Irikura, V., Yamaguchi, S., DeRosier, D., and Macnab, R. (1992) Localization of the *Salmonella typhimurium* flagellar switch protein FliG to the cytoplasmic M-ring face of the basal body. *Proc Natl Acad Sci USA* **89:** 6304–6308.

Frankel, G., Phillips, A.D., Rosenshine, I., Dougan, G., Kaper, J.B., and Knutton, S. (1998) Enteropathogenic and enterohaemorrhagic *Escherichia coli*: more susbversive elements. *Mol Microbiol* **30:** 911–921.

Galan, J.E., Ginocchio, C., and Costeas, P. (1992) Molecular and functional characterization of the *Salmonella* invasion gene *invA*: homology of InvA to members of a new protein family. *J Bacteriol* **174:** 4338–4349.

Gauthier, A., Puente, J., and Finlay, B. (2003) Secretin of the enteropathogenic *Escherichia coli* type III secretion system requires components of the type III apparatus for assembly and localization. *Infect Immun* **71:** 3310–3319.

Gennity, J., and Inouye, M. (1991) The protein sequence responsible for lipoprotein membrane localization in *Escherichia coli* exhibits remarkable specificity. *J Biol Chem* **266:** 16458–16464.

Gennity, J., Kim, H., and Inouye, M. (1992) Structural determinants in addition to the amino-terminal sorting sequence influence membrane localization of *Escherichia coli* lipoproteins. *J Bacteriol* **174:** 2095–2101.

Hayashi, S., and Wu, H. (1990) Lipoproteins in bacteria. *J Bioenerg Biomembr* **22:** 451–471.

Hensel, M., Shea, J.E., Raupach, B., Monack, D., Falkow, S., Gleeson, C., *et al.* (1997) Functional analysis of *ssaJ* and the *ssaK/U* operon, 13 genes encoding components of the type III secretion apparatus of *Salmonella* Pathogenicity Island 2. *Mol Microbiol* **24:** 155–167.

Holm, L., and Sander, C. (1993) Protein structure comparison by alignment of distance matrices. *J Mol Biol* **233:** 123–138.

Hueck, C.J. (1998) Type III protein secretion systems in bacterial pathogens of animals and plants. *Microbiol Mol Biol Rev* **62:** 379–433.

Jarvis, K.G., Giron, J.A., Jerse, A.E., McDaniel, T.K., Donnenberg, M.S., and Kaper, J.B. (1995) Enteropathogenic *Escherichia coli* contains a putative type III secretion system necessary for the export of proteins involved in attaching and effacing lesion formation. *Proc Natl Acad Sci USA* **92:** 7996–8000.

Jouihri, N., Sory, M., Page, A., Gounon, P., Parsot, C., and Allaoui, A. (2003) MxiK and MxiN interact with the Spa47 ATPase and are required for transit of the needle components MxiH and MxiI, but not of Ipa proteins, through the type III secretion apparatus of *Shigella flexneri*. *Mol Microbiol* **49:** 755–767.

Juncker, A.S., Willenbrock, H., Von Heijne, G., Brunak, S., Nielsen, H., Krogh, A. (2003) Prediction of lipoprotein signal peptides in gram-negative bacteria. *Protein Sci* **12:** 1652–1662.

Kihara, M., Miller, G., and Macnab, R. (2000) Deletion analysis of the flagellar switch protein FliG of *Salmonella*. *J Bacteriol* **182:** 3022–3028.

Kimbrough, T.G., and Miller, S.I. (2000) Contribution of *Salmonella typhimurium* type III secretion components to needle complex formation. *Proc Natl Acad Sci USA* **97:** 11008–11013.

Knutton, S., Lloyd, D.R., and McNeish, A.S. (1987) Adhesion of enteropathogenic *Escherichia coli* to human intestinal enterocytes and cultured human intestinal mucosa. *Infect Immun* **55:** 69–77.

Knutton, S., Baldwin, T., Williams, P.H., and McNeish, A.S. (1989) Actin accumulation at sites of bacterial adhesion to tissue culture cells: basis of a new diagnostic test for enteropathogenic and enterohemorrhagic *Escherichia coli*. *Infect Immun* **57:** 1290–1298.

Knutton, S., Rosenshine, I., Pallen, M.J., Nisan, I., Neves, B.C., Bain, C., *et al.* (1998) A novel EspA-associated surface organelle of enteropathogenic *Escherichia coli* involved in protein translocation into epithelial cells. *EMBO J* **17:** 2166–2176.

Koster, M., Bitter, W., de Cock, H., Allaoui, A., Cornelis, G.R., and Tommassen, J. (1997) The outer membrane component, YscC, of the Yop secretion machinery of *Yersinia enterocolitica* forms a ring-shaped multimeric complex. *Mol Microbiol* **26:** 789–797.

Kubori, T., Matsushima, Y., Nakamura, D., Uralil, J., Lara-Tejero, M., Sukhan, A., *et al.* (1998) Supramolecular structure of the *Salmonella typhimurium* type III protein secretion system. *Science* **280:** 602–605.

Kubori, T., Sukhan, A., Aizawa, S.I., and Galan, J.E. (2000) Molecular characterization and assembly of the needle complex of the *Salmonella typhimurium* type III protein secretion system. *Proc Natl Acad Sci USA* **97:** 10225–10230.

Levine, M.M., Nataro, J.P., Karch, H., Baldini, M.M., Kaper, J.B., Black, R.E., *et al.* (1985) The diarrheal response of humans to some classic serotypes of enteropathogenic *Escherichia coli* is dependent on a plasmid encoding an enteroadhesiveness factor. *J Infect Dis* **152:** 550–559.

Macnab, R.M. (2003) How bacteria assemble flagella. *Annu Rev Microbiol* **57:** 77–100.

Macnab, R.M. (2004) Type III flagellar protein export and flagellar assembly. *Biochim Biophys Acta* **1694:** 207–217.

Marenne, M., Journet, L., Mota, L., and Cornelis, G. (2003) Genetic analysis of the formation of the Ysc–Yop translocation pore in macrophages by *Yersinia enterocolitica*: role of LcrV, YscF and YopN. *Microb Pathog* **35:** 243–258.

Marlovits, T.C., Kubori, T., Sukhan, A., Thomas, D.R., Galan, J.E., and Unger, V.M. (2004) Structural insights into the assembly of the type III secretion needle complex. *Science* **306:** 1040–1042.

Marykwas, D., Schmidt, S., and Berg, H. (1996) Interacting components of the flagellar motor of *Escherichia coli* revealed by the two-hybrid system in yeast. *J Mol Biol* **256:** 564–576.

McDaniel, T.K., Jarvis, K.G., Donnenberg, M.S., and Kaper, J.B. (1995) A genetic locus of enterocyte effacement conserved among diverse enterobacterial pathogens. *Proc Natl Acad Sci USA* **92:** 1664–1668.

Matsuzawa, T., Kuwae, A., Yoshida, S., Sasakawa, C., and Abe, A. (2004) Enteropathogenic *Escherichia coli* activates the RhoA signaling pathway via the stimulation of GEF-H1. *EMBO J* **23:** 3570–3582.

Michiels, T., Vanooteghem, J.C., Lambert de Rouvroit, C., China, B., Gustin, A., Boudry, P., and Cornelis, G.R. (1991) Analysis of *virC*, an operon involved in the secretion of Yop proteins by *Yersinia enterocolitica*. *J Bacteriol* **173:** 4994–5009.

Mounier, J., Bahrani, F.K., and Sansonetti, P.J. (1997) Secretion of *Shigella flexneri* Ipa invasins on contact with epithelial cells and subsequent entry of the bacterium into cells are growth stage dependent. *Infect Immun* **65:** 774–782.

Mundy, M., Petrovska, L., Smollett, K., Simpson, N., Wilson, R.K., Yu, J., *et al.* (2004) Identification of a novel *Citrobacter rodentium* type III secreted protein, EspI, and the roles of this and other secreted proteins in infection. *Infect Immun* **72:** 2288–2302.

Nataro, J.P., and Kaper, J.B. (1998) Diarrheagenic *Escherichia coli*. *Clin Microbiol Rev* **11:** 142–201.

Neves, B.C., Shaw, R.K., Frankel, G., and Knutton, S. (2003) Polymorphisms within EspA filaments of enteropathogenic and enterohemorrhagic *Escherichia coli*. *Infect Immun* **71:** 2262–2265.

Oosawa, K., Ueno, T., and Aizawa, S. (1994) Overproduction of the bacterial flagellar switch proteins and their interactions with the MS ring complex *in vitro*. *J Bacteriol* **176:** 3682–3691.

Saijo-Hamano, Y., Uchida, N., Namba, K., and Oosawa, K. (2004) *In vitro* characterization of FlgB, FlgC, FlgF, FlgG, and FliE, flagellar basal body proteins of *Salmonella*. *J Mol Biol* **339:** 423–435.

Sankaran, K., and Wu, H. (1994) Lipid modification of

bacterial prolipoprotein. Transfer of diacylglyceryl moiety from phosphatidylglycerol. *J Biol Chem* **269:** 19701–19706.

Sattler, M., Schleucher, J., and Griesinger, C. (1999) Heteronuclear multidimensional NMR experiments for the structure determination of proteins in solution employing pulsed field gradients. *Prog NMR Spect* **34:** 93–158.

Schlosser-Silverman, E., Elgrably-Weiss, M., Rosenshine, I., Kohen, R., and Altuvia, S. (2000) Characterization of *Escherichia coli* DNA lesions generated within J774 macrophages. *J Bacteriol* **182:** 5225–5230.

Schuch, R., and Maurelli, A.T. (2001) MxiM and MxiJ, base elements of the Mxi-Spa type III secretion system of *Shigella*, interact with and stabilize the MxiD secretin in the cell envelope. *J Bacteriol* **183:** 6991–1998.

Seydel, A., Gounon, P., and Pugsley, A. (1999) Testing the '+2 rule' for lipoprotein sorting in the *Escherichia coli* cell envelope with a new genetic selection. *Mol Microbiol* **34:** 810–821.

Sukhan, A., Kubori, T., Wilson, J., and Galan, J.E. (2001) Genetic analysis of assembly of the *Salmonella enterica* serovar Typhimurium type III secretion-associated needle complex. *J Bacteriol* **183:** 1159–1167.

Sukhan, A., Kubori, T., and Galan, J. (2003) Synthesis and localization of the *Salmonella* SPI-1 type III secretion needle complex proteins PrgI and PrgJ. *J Bacteriol* **185:** 3480–3483.

Tamano, K., Aizawa, S., Katayama, E., Nonaka, T., Imajoh-Ohmi, S., Kuwae, A., *et al.* (2000) Supramolecular structure of the *Shigella* type III secretion machinery: the needle part is changeable in length and essential for delivery of effectors. *EMBO J* **19:** 3876–3887.

Tampakaki, A., Fadouloglou, V., Gazi, A., Panopoulos, N., and Kokkinidis, M. (2004) Conserved features of type III secretion. *Cell Microbiol* **6:** 805–816.

Ueno, T., Oosawa, K., and Aizawa, S. (1992) M ring, S ring and proximal rod of the flagellar basal body of *Salmonella typhimurium* are composed of subunits of a single protein, FliF. *J Mol Biol* **227:** 672–677.

Ueno, T., Oosawa, K., and Aizawa, S. (1994) Domain structures of the MS ring component protein (FliF) of the flagellar basal body of *Salmonella typhimurium*. *J Mol Biol* **236:** 546–555.

Wilson, R.K., Shaw, R.K., Daniell, S., Knutton, S., and Frankel, G. (2001) Role of EscF, a putative needle complex protein, in the type III protein translocation system of enteropathogenic *Escherichia coli*. *Cell Microbiol* **3:** 753–762.

Yahr, T.L., Goranson, J., and Frank, D.W. (1996) Exoenzyme S of *Pseudomonas aeruginosa* is secreted by a type III pathway. *Mol Microbiol* **22:** 991–1003.